Rev. Roum. Sci. Techn.– Électrotechn. et Énerg.
Vol. **71**, *2*, pp. 287–292, Bucarest, 2026

COMPARISON OF FRACTIONAL ORDER PID AND PID CONTROLLERS: A NOVEL TUNING METHOD AND PERFORMANCE ANALYSIS

ANBUMANI KUMARASAMY[1], SUJIT KUMAR[2], KOMALA CHOWDENAHALLY RAMASWAMY[3], MADHANA MOHAN KANNAN[1]

Keywords: PID controller; Optimization; Control system robustness; Edge compensation; Fractional-order system.

This study presents a direct comparison between fractional-order PID (FOPID) and classical PID controllers using a novel regularization-based tuning technique originally developed for integral-order controllers and adapted for fractional-order applications. Although the optimization problem is not convex by its nature, the objective function sweep results indicate the weak convexity of the problem, which validates the proposed method. Simulation results illustrate that the integral order (λ) is typically close to 1, which suggests that there is little advantage in integrating the fractional order in the conventional case. But improvements were noted in systems with positive zeros (far from the origin), long dead times, and high order. In these cases, FOPID carriers reduced ITAE by 20–30%, reduced settling time by 10–30%, and increased phase margin by up to 30%, further demonstrating better performance and robustness. The advantages stem from the softer polynomial kernel of the fractional derivative, which provides more flexible control in systems with intricate or suspended dynamics than that of classical PID controllers.

1. INTRODUCTION

The fractional order PID (FOPID) controller, also known as $PI^{\lambda}D^{\mu}$, is the generalization of the classical PID controller to non-integer orders of integration and differentiation, giving more degrees of freedom for tuning and better control performance for complicated processes [1]. Due to this added degree of freedom, fractional order control was shown to be of great interest for the applications that ask for improved dynamic response, higher robustness, and better stability. Similar control advances have also been observed in modified PID liquid-level systems [2], robust design of power system stabilizer (PSS) based on [3], application [4] to induction heating, and application [5] to DC machine motor drives.

High-order FOPID and other formerly inaccessible control techniques have recently been applied to a wide variety of systems. AI-based techniques have been studied for nonlinear reactor dynamics [6], dual fuzzy technique for enhanced power quality control [7], Smith-predictor-based FOPID for the delay-dominated solar collector fields [8], tuning based on metaheuristics for an enhanced control of the rotary inverted pendulum [9], and hybrid optimization for the UAV path-planning control with FOPID-TID structures [10]. Further enhancements have been described in predictive control of inverted pendulum systems [11], robust fractional order buck–boost converter control [12], and switched mode PID compensation in the presence of actuator nonlinearities [13]. Decision-tree logic enhanced the Fuzzy-PID tuning [14], ANN-PID was implemented for solar tracking [15], and GA/neuro-fuzzy techniques were applied for PI speed control of the motor [16]. They also reported sliding mode control tracking for PMSM drives [17], Aquila-optimized control for boost converters [18], stable robust microgrid control [19], wind-power control via sliding/backstepping/fuzzy techniques [20], adaptive predictive inverter control [21], and real-time synergetic boost-converter regulation [22].

In contrast to the literature, where tuned methods for PID and FOPID controllers are different, here we propose one regularization-based tuning method that can be applied to both controller types. As a result, a fair comparison is ensured, and the natural merits of fractional-order control can be brought out with the same design specifications. In this paper, a general and structured tuning approach to both conventional PID and fractional-order PID (FOPID) controllers is presented. This provides a consistent design procedure for the controllers and an equal footing for performance comparison between them.

2. FREQUENCY DOMAIN CONTROLLER ADJUSTMENT

The FOPID controller (Fig. 2) used in this study is different from the traditional controller (Fig. 1) commonly found in the literature.

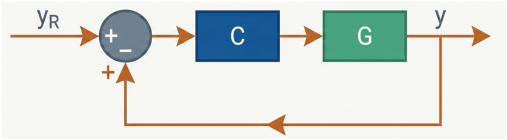

Fig. 1 – Traditional controller.

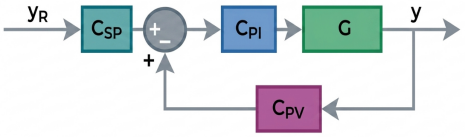

Fig. 2 – FOPID controller.

The standard PID controller is depicted in Fig. 1, and the fractional-order PID (FOPID) controller considered in this work is shown in Fig. 2. As the latter generalizes the classic structure by adding fractional integral and derivative orders, it has more degrees of freedom for tuning. Its structure is shown in Equation 1, where the control signal $\Delta U(s)$ is a function of the difference between $\Delta Y_r(s)$, $Y(s)$ and $\Delta Y(s)$, which is the output of the reference process. The controller combines proportional, fractional integral (λ), and fractional derivative (μ) functions and has the following settings: proportional gain (K_c), integral time (T_i), generation time (T_d), and derivative filtering (N).

$$\Delta U(s) = K_c\left[\left(\Delta Y_r(s) - \Delta Y(s)\right) + \frac{1}{T_i s^{\lambda}}\left(\Delta Y_r(s) - \right.\right.$$
$$\left.\left. -\Delta Y(s)\right) + \frac{T_d s^{\mu}}{\frac{T_d}{N}s^{\mu}+1}\left(-\Delta Y(s)\right)\right]. \quad (1)$$

This tuning scheme was originally designed for small

[1] Department of Electronics and Instrumentation Engineering, Sri Sairam Engineering College, Chennai. Tamil Nadu 600044, India.
[2] Department of Electrical and Electronics Engineering, Amrita Vishwa Vidyapeetham, Bengaluru, India.
[3] Department of Computer Science and Engineering (IoT&CSBT), East Point College of Engineering and Technology, Bidarahalli, Bengaluru, Karnataka 560049, India.
Emails: anbumani.ei@srm.edu.in, sujit-eee@dayanandasagar.edu, nandaashwin@eastpoint.ac.in, madhanamohan.ei@sairam.edu.in

DOI: 10.59277/RRST-EE.2026.2.20

controllers based on response approximation. To cope with nonconvexity and final convergence, in [4], we propose a structured iterative scheme that decomposes the optimization into two subproblems based on a two-degree-of-freedom (2DOF) control loop. Move to this line for the FOPID control setup.

2.1 TWO-DEGREE-OF-FREEDOM LOOP

A classical control system is based on the well-known feedback loop, and this classical loop can be modified to a two-degree-of-freedom control, where the control effort is separately influenced by the reference and the plant output. Two nested filters are involved, the state filter (C_{SP}) and the process variable filter (C_{PV}), and the primary controller (C_{PI}) is implemented here as the FOPI controller described in eq. (2)-(4).

$$C_{PI} = K_c.\left(1+\frac{1}{T_i s^{\lambda}}\right). \tag{2}$$

2.2 CONVERSION TO 2DOF STRUCTURE

In terms of block algebra, the initial FOPID block has a 2DOF line. This yields the filters (C_{SP} and C_{PV}) as a function of the FOPID parameters.

$$C_{SP} = \frac{1}{C_{PI}}.\frac{\Delta U(s)}{\Delta Y_r(s)}, \tag{3}$$

$$C_{PV} = -\frac{1}{C_{PI}}.\frac{\Delta U(s)}{\Delta Y(s)}. \tag{4}$$

In the controller of this study, C_{SP} is equal to 1, and C_{PV} is expressed as a rational function of the crushing force.

$$C_{PV} = \frac{\left(1+\frac{1}{N}\right)T_i T_d s^{\lambda+\mu}+T_i s^{\lambda}+\frac{T_d}{N}s^{\mu}+1}{\frac{T_i T_d}{N}s^{\lambda+\mu}+T_i s^{\lambda}+\frac{T_d}{N}s^{\mu}+1}. \tag{5}$$

2.3 SEQUENTIAL ITERATIVE OPTIMIZATION METHOD (SIOM)

Controller tuning is formulated as a frequency-domain optimization problem, eq. (6) and eq. (7), with the primary goal of minimizing the distance between the actual and desired loop responses. Because of the nonconvexity of the problem, it is solved by iterations:

- Iteration 1, Step 1: Using the unit filter, estimate the FOPI parameters (K_c, T_i, λ).
- Iteration 1, Step 2: Adjust the previous parameters and estimate the remaining FOPID parameters (T_d, μ).
- Subsequent iterations: Estimate two parameters and change the filter and controller until the maximum limit of convergence or iteration is reached.

$$\min_{x\in R^+} FO(x) = \sum_{s=j\omega_0}^{j\omega_1}\left|\left(T(s,x)-T_0(s).\frac{1}{s}\right)^2\right| \tag{6}$$

$$FO(x) = \sum_{s=j\omega_0}^{j\omega_1}\left|\left(\frac{G(s)C_{PI}(s)(C_{SP}(s,x)-T_0(s)C_{PV}(s,x)-T_0(s)}{1+G(s)C_{PI}(s,x)C_{PV}(s,x)}.\frac{1}{s}\right)^2\right| \tag{7}$$

Convergence is determined by the relative error between parameters in consecutive iterations with a threshold of 1%.

$$|\text{error}[x_i]| = \left|\frac{x_i^{nit}-x_i^{nit-1}}{x_i^{nit}}\right|.100\% \le \varepsilon, \quad i = 1,2,3,4,5 \tag{8}$$

2.4 ACHIEVABLE PERFORMANCE FUNCTION (APF)

APF makes a perfect closed-loop response, and it should be properly selected according to the plant dynamics. The APFs introduced in this paper are derived from the TTTs, which are optimal w.r.t. the ITAE criterion. These functions are parameterized in order (m) and natural frequency (ω_n) and possess steady-states, no steady-state error, and fast steady-states. If the plant contains nominal phase elements or dead times, then modifications are required for the internal stability.

2.5. OBJECTIVE FUNCTION SWEEP

This section derives the optimization problem in standard form to solve the non-convex minimization Problem (5) by using the Goal Attain method based on sequential quadratic programming. Since FOPID tuning is also frequently stated to be strongly non-convex, some objective-function scans were conducted to confirm the appropriateness of the used optimization procedure.

To this end, the proposed tuning method was applied to fixed values of λ and μ in the intervals (0.8; 1.2) and (0.4; 1.8), respectively, spaced apart by the value of 0.025. For each pair λ and μ, a three-dimensional graph was made with the value of the objective function on the Z axis, and the values of λ and μ, ε on the X and Y axes, respectively.

This procedure was applied to four plants to confirm the presence of local minima in the objective function. The plants considered are described by the following transfer functions, eq. (9)-(12).

$$G1(s) = \frac{e^{-1.s}}{3.s^2+1.s+1}, \tag{9}$$

$$G2(s) = \frac{e^{-1.s}.(1-2.s)}{(4.s^2+2.s+1).(2.s+1)}, \tag{10}$$

$$G3(s) = \frac{e^{-1.s}}{(3.s^2+4.s+1).(1.5.s^2+1.s+1)}, \tag{11}$$

$$G4(s) = \frac{1.5.s^5+4.s^4+8.5.s^3+4.5.s^2+1.667.s+0.5556}{6.s^6+23.s^5+38.s^4+34.67.s^3+18.11.s^2+5.s+0.5556}. \tag{12}$$

In all four cases, the same desired performance function was chosen, as given by

$$T_0(s) = \frac{0.1717}{s^2+0.5801.s+0.1717} \tag{13}$$

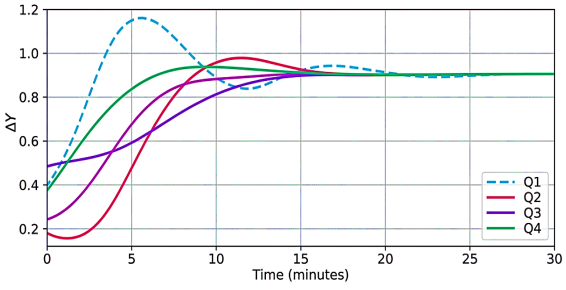

Fig. 3 – Step responses of the transfer functions G1, G2, G3, G4, and T0.

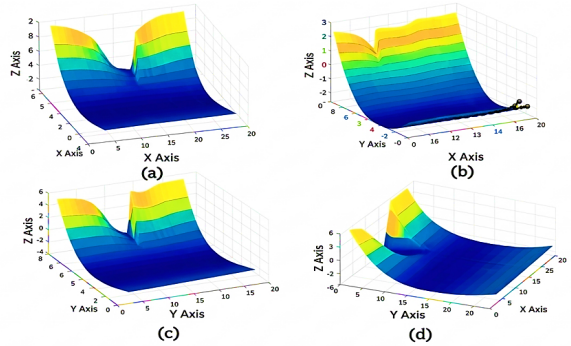

Fig. 4 – Objective function scan for plants: (a) G1; (b) G2; (c) G3, and (d) G4.

The responses to step inputs of each plant and the FDA are depicted in Fig. 3, and the associated sweep plots of the objective functions are presented in Fig. 4.

It is important to mention that the FDA in the above figure does not consider the non-minimum phase terms were multiplied, which are distinct for each plant.

From Fig. 4, we observe that at least in this case, non-convexity is rather mild. Although this certainly does not guarantee that any plant and desired performance will not lead to local minima, it is quite an indication that, in general, these will not be a problem; they would have to be quite "deep" (more precisely, multiple local minima) to motivate the use of methods such as particle scanning or genetic algorithms. Smoothness is another important aspect when describing an objective function and is extremely helpful, for instance, in derivative-based methods such as the sequential quadratic programming (SQP) applied in this work. Therefore, it is the system can be considered the tuning approach presented here is suitable for FOPID controllers.

3. CASE STUDIES

This paper relies on simulation studies performed in MATLAB/Simulink, allowing us to assess the performance and the robustness of different plant classes in a controlled environment. The aforementioned tuning approach was applied to tune FOPID and PID controllers for multiple scenarios to make a comparison. The employed PID controller is represented as eq. (1).

Clearly, this controller is a special case of the controller in (5) when the integral and derivative orders are both set to one. The investigation was carried out by simulating four different categories of plants in a closed loop: underdamped, with positive zeros, with high dead time, and high-order. In each case, performance and robustness measures were computed for the two controller-based control loops to determine in which cases the FOPID controller provides improvements over the PID.

All simulations were done in MATLAB/Simulink. Simulations of fractional order systems were done using the fractional order modeling and control (FOMCON) toolbox, as explained in [17]. The fractional operator is approximated by the fifth-order Oustaloup recursive filter in the frequency band (0.0001; 10000).

The models used to conduct the tests with the corresponding closed-loop system specifications in each case will be shown below. For each transfer function given a FOPID and a PID controller were designed using according the procedure given in previous section and the following performance indices were computed: settling time (tA, for a range of 5% above or below the final response) and the integral of the time weighted absolute error (ITAE), besides the robustness indices: maximum sensitivity (MS), gain margin (MG) and phase margin (PM).

3.1. UNDERDAMPED PLANTS (CASE A)

The first series of simulations aimed to verify whether the FOPID controller offers advantages when used to control underdamped plants, i.e., with a damping factor (ζ) lower than unity. The plant model used in the tests is given below, eq. (15), as well as the values of ζ used.

$$G = \frac{1}{(100.s^2+20\,\zeta s+1)}.\mathrm{e}^{-s}, \quad \zeta = 1; 0.7; 0.4; 0.1 \qquad (14)$$

A first-order FDA was chosen for all cases, with a settling time equal to 60% of the plant settling time. This information is summarized in Table 1.

3.2. PLANTS WITH POSITIVE ZEROS (CASE B)

Here, it was verified whether the FOPID controller offers advantages when used to control plants with positive zeros, related to the parameter β, the time constant of the numerator. Such plants present an inverse response that increases with the increase in the magnitude of β. The plant model used in the simulations is given in eq. (15), as well as the values β used,

$$G = \frac{(-\beta s + 1)}{(10s+1)^3}.\mathrm{e}^{-s}, \quad \beta = 5; 10; 15; 20. \qquad (15)$$

A second-order FDA was chosen for all cases, with a settling time equal to one-third of the plant settling time. This information is summarized in Table 1.

3.3. PLANTS WITH HIGH DEAD TIME (CASE C)

In these simulations, it was verified how the FOPID controller changes the behavior of the closed loop when the plant presents high dead time (θ). The plant model used in the simulations is given in eq. (16), as well as the values θ used.

$$G = \frac{1}{(10.s+1)^3}\mathrm{e}^{-\theta.s}, \qquad \theta = 3; 6; 9; 12. \qquad (16)$$

In all these cases, the plant settling time was taken as the characteristic settling time minus dead time of each case. A second-order FDA was selected for all cases, with a settlement time set equal to 40% of the plant settlement time for the first two cases, and 50% for the other two cases. This is the summary of Table 2.

3..4. HIGHER ORDER PLANTS (CASE D)

In the latter scenario, the potential superiority of the FOPID controller over the PID one was investigated when the controlled plant is of high order. The plant model used for the simulations is at eq. (17), as well as the orders (n) used.

$$G = \frac{1}{(10.s+1)^n}.e^{-1.s}, \qquad n = 3; 4; 5; 6. \qquad (17)$$

Table 1

Plants and the FD were used in case A and case B.

Case A			Case B		
Model		FDA (m=1)	Model		FDA (m=2)
Case	$tA\,(min)$	$tA\,(min)$	Case	$tA\,(min)$	$tA\,(min)$
A1 (ζ=1)	47.55502	26.57502	B1 (β=5)	66.00502	20.41502
A2 (ζ=0.7)	29.11502	15.51502	B2 (β=10)	68.30502	21.17502
A3 (ζ=0.4)	76.19502	43.76502	B3 (β=15)	69.75502	21.66502
A4 (ζ=0.1)	289.665	171.845	B4 (β=20)	70.75502	21.99502

Table 2

Plants and FDA used in case C and case D.

Case C			Case D		
Model		FDA (m=1)	Model		FDA (m=2)
Case	$tA\,(min)$	$tA\,(min)$	Case	$tA\,(min)$	$tA\,(min)$
C1 θ=3)	64.07502	23.29502	D1 (n=3)	63.96 (m=2)	25.18
C2 (θ=6)	67.07502	23.29502	D2 (n=4)	78.54 (m=3)	38.77
C3 (θ=9)	70.07502	29.59502	D3 (n=5)	92.54 (m=4)	54.92
C4 (θ=12)	73.07502	29.59502	D4 (n=6)	106.13 (m=5)	63.08

For all cases, an FDA of one order lower than the plant order was selected, and the settling time was set equal to 40% and 50% of the plant settling time for the first two cases, and 60% for the last two, respectively. This is the

information according to Table 2.

4. RESULTS AND DISCUSSION

The simulation results for the proposed case studies are summarized in Fig. 5, which shows the tuned PID and FOPID controller parameters and the final objective-function values (FO). From the comparison of the final FO, it can be seen that A4 is the only subcase where the FOPID controller is not able to obtain a lower value of the objective function than the PID controller. Otherwise, FOPID produces a smaller final FO, which means the fractional derivative term offers an extra degree of flexibility for the realization of the given closed-loop performance specification.

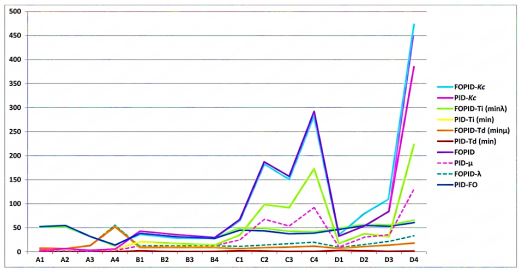

Fig. 5 – Comparison of the tuning results of the PID and FOPID for sub-cases A1–D4 including the controller parameters (K_c, T_i, T_d, λ, μ), and the final values of objective-function (FO).

In addition, the parameter λ converged to unity in all the cases, indicating that the fractional-order integral action does not have an evident benefit compared to the integer-order integral action in the considered scenarios. Such observations were reported in [11–13].

Nevertheless, this has resulted in the FDA definition, because all the case studies consider integer-order transfer functions. As for the other parameters, in Case A, the fractional derivative order μ is close to unity, and the controller gains and time constants of the FOPID and PID controllers are very close. μ takes on values in the other three cases about 10% to 15% greater than unity, and T_d in the FOPID controller is about 20% to 80% larger than that of the PID controller. The rest of the parameters also turned out to be slightly higher in the FOPID controller, yet these increments were all below 10% approximately [17–22].

Figure 6 plots the performance and robustness of PID and FOPID for all the subcases. ITAE, tA, MS, MG, and RF are in Fig. 6. The two controllers are almost identical in Case A, and more evident differences arise in Cases B, C and D, where FOPID typically yields smaller ITAE and settling time. In terms of robustness, MG is barely influenced, MS is slightly enhanced, and the major gain is found in RF particularly in Cases C and D. In general, FOPID is more favorable in the case of a large dead time and high order plant.

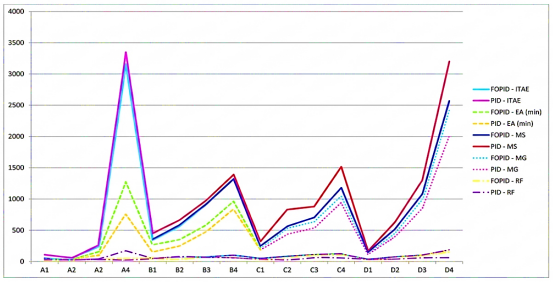

Fig. 6 – Performance and robustness indices of PID and FOPID control loops for different subcases A1–D4.

For Case A, the two controllers had similar performance and robustness, as expected given the closeness of their parameter values. In the other cases, the differences were more striking, as shown in Fig. 7 by the FOPID-to-PID criterion ratios. The gain margin was omitted because it was virtually the same for the two controllers, with a maximum difference of 5.2%. In Fig. 7, the FOPID controller reduced the ITAE and the settling time in subcase A2 and in Cases B, C and D. The biggest decreases in ITAE were found in Cases C and D (also a significant decrease in B1), while the best improvements in settling time were found in B1, B2, and C1.

In Case A, there was enhancement only at A2, which may well be due to that the chosen FDA was simpler to meet. Regarding robustness, gain margin remained almost the same, and maximum sensitivity got somewhat better — only in the sense that a small reduction was observed in A2.

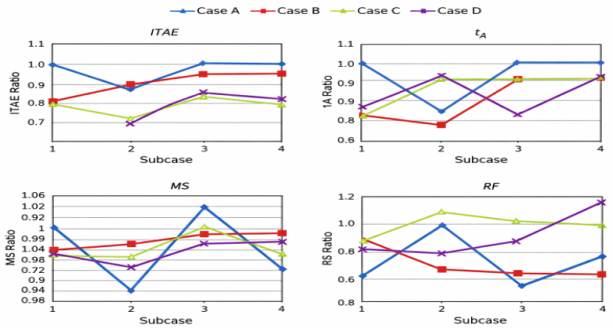

Fig. 7 – Ratio between the criteria calculated for FOPID controllers and PID controllers as a function of the subcase.

The largest improvement in robustness was attained by RF, which also increased in A2 and B1, with the largest increase, almost 30%, at D4, and in Cases C and D. For Case B, the improvement in ITAE and RF was more pronounced in the 1st subcase, and the maximal reduction in settling time appeared in the 2nd subcase. In general, the highest gains of FOPID were reached in Cases C and D, which implies that high dead time, high-order plants could gain the most from fractional-order control.

In the subsequent subcases, the best results for ITAE and RF were obtained in Cases C and D for the FOPID controller, which suggests that plants with large dead time and high order are likely to get the largest benefits from fractional-order control.

As a result of the demonstrated improved performance, for this situation, responses to unit step disturbances in the reference variable are illustrated in Figs. 8, 9, 10, and 11 for case C and in Figs. 12, 13, 14, and 15 for case D to facilitate the observation. Also shown are the manipulated variable responses.

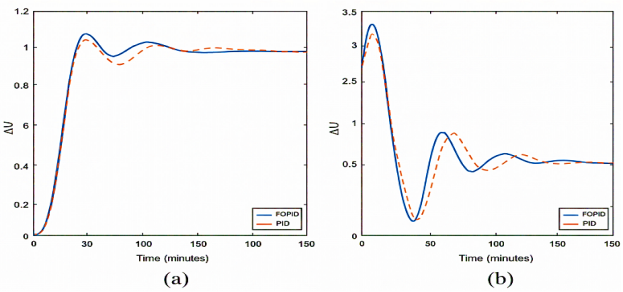

Fig. 8 – Step response of loop C for θ = 3: (a) regulated variable and (b) adjustment action

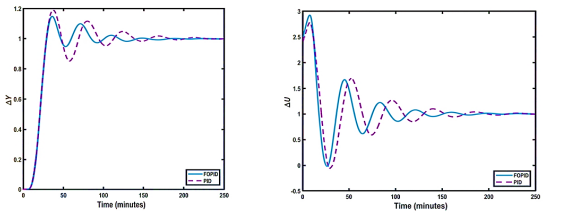

Fig. 9 – Step response of loop *C* for θ = 6: (a) regulated variable and (b) adjustment action

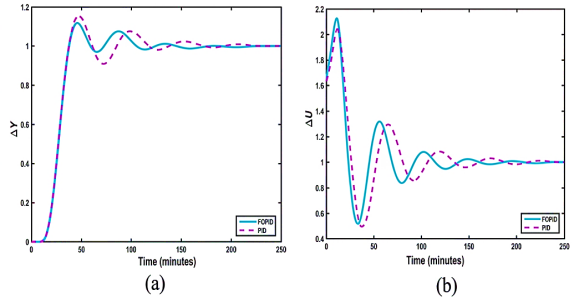

Fig. 10 – Step response of loop *C* for θ = 9: (a) regulated variable and (b) adjustment action

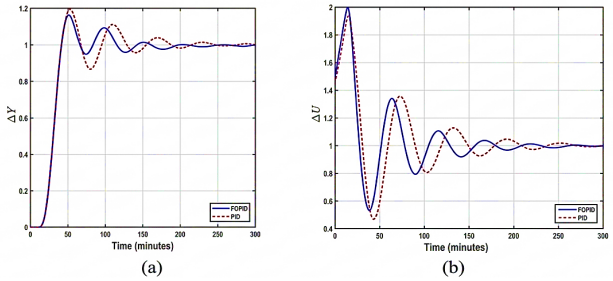

Fig. 11 – Step response of loop *C* for θ = 12: (a) regulated variable and (b) adjustment action

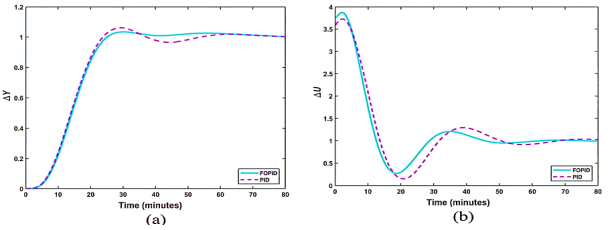

Fig. 12 – Step response of the *D*-loop for n = 3: (a) regulated variable and (b) adjustment action

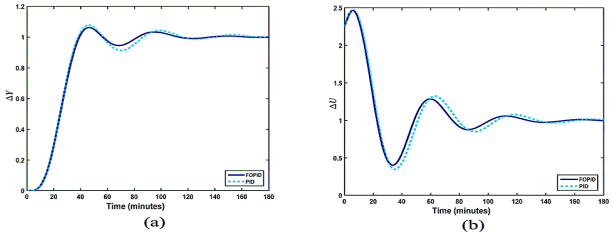

Fig. 13 – Step response of the D loop for n = 4: (a) regulated variable and (b) adjustment action.

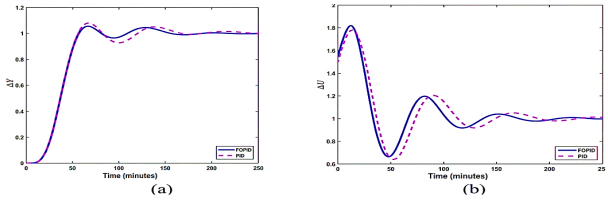

Fig. 14 – Step response of the D-loop for n = 5: (a) regulated variable, and (b) adjustment action.

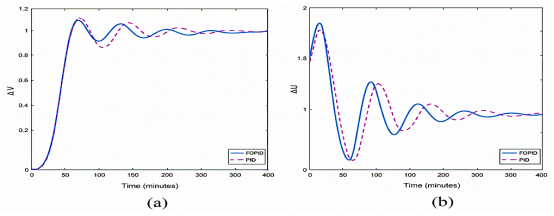

Fig. 15 – Step response of the D loop for n = 6: (a) regulated variable, and (b) adjustment action.

Experimental results show that FOPID controllers provide better performance than classical PID structures in the case of systems with complex phase characteristics and nonlinear dynamic behaviors. This can be seen from the development in smart LED drivers, where FOPID can reduce oscillations [1] and the improved robustness of the three-tank liquid level system with modified PID controllers [2]. Such robustness is also essential for power system stabilizers [3] and for eliminating dead time in induction heating inverters [4], as well as for synergetic speed control in induction motor drives [5]. Although artificial intelligence is used to monitor nonlinear chemical reactor processes [6], the power quality in PV-integrated systems can be enhanced with a dual fuzzy-Sugeno method [7]. The effectiveness of FOPID is also reported in solar collector fields using filtered Smith predictors [8] and in metaheuristic-optimized rotary inverted pendulum [9], in which it reduces settling time and ITAE. In addition, hybrid optimization for UAV path planning [10] and predictive control for inverted pendulums [11] underline the versatility of the contemporary control paradigm. Similarly, optimal FOPID is used for buck-boost converters [12], and switched-mode PID is used to o compensate for backlash [13]. In the case of fuzzy-PID in conjunction with decision trees [14] or neural networks in solar tracking [15], the researchers are going beyond the basic tuning, similar to the neuro-fuzzy speed controllers for dual star induction motors [16]. Better transient responses are also reported in sliding mode controlled synchronous permanent motor drives [17] and Aquila-based DC-DC converters [18]. Finally, the systematic framework to perform an in-depth comparison between fractional-order and conventional control approaches is given by hybrid sliding mode control for microgrids [19], wind power backstepping control [20], adaptive observers for model-free predictive control [21], and synergetic regulators for boost converters [22].

6. CONCLUSIONS

In the present work, a unified tuning rule for the PID or FOPID controller was introduced, enabling a performance comparison. Although some doubt existed beforehand, the sweeps of the objective function confirmed the approach's adequacy despite its nonconvexity. Simulation results demonstrated that, in the majority of the cases, FOPID was not applicable because the integral order λ was approximated to 1 (integer value). However, for plants with long life, positive zeros (away from the source) or high levels, FOPID overestimated PID—20–30 % smaller ITAE, 10–30 % smaller steady-state time, and as much as 30 % easier to control. Such effects are credited to the fractional derivative μ, which enhances the flexibility and robustness of the tuning, particularly in complex dynamical systems. The suggested tuning method could be an attractive alternative to existing methods, especially for systems with complex dynamics, *e.g.*,

dead time, non-minimum-phase, and high-order systems. The various case studies clearly show that it can be successfully applied to many practical control problems. While the current investigation is supported by simulation results, future work will focus on real-time experimental verification using hardware platforms, such as an embedded controller or a laboratory-scale process system, to further assess the practicality of the proposed tuning scheme.

ACKNOWLEDG(E)MENTS

The authors would like to thank their supervisor and their Institution for enabling this research to be successfully conducted.

CREDIT AUTHORSHIP CONTRIBUTION STATEMENT

ANBUMANI KUMARASAMY: Conceptualization, Methodology, Software, Formal analysis, Investigation, Writing – original draft.
SUJIT KUMAR: Data curation, Validation, Visualization, Writing – review & editing.
KOMALA CHOWDENAHALLY RAMASWAMY: Supervision, Resources, Project administration, Writing – review & editing.
MADHANA MOHAN KANNAN: Conceptualization, Methodology, Supervision, Funding acquisition, Writing – review & editing.

Received on 28 June 2025

REFERENCES

1. G. Murugaiyan, J. Gnanamalar, M. Narayanaperumal, V. Muthuvel, *Red fox-based fractional order fuzzy PID controller for smart LED driver circuit*, Rev. Roum. Sci. Techn. – Électrotechn. et Énerg., **68**, *4*, pp. 394–399 (2023).
2. A. Idir, M. Nesri, K. Belhouchet, S. Guedida, L. Canale, *Enhancing the transient performances and stability of three-tank liquid level using a modified PID controller*, Rev. Roum. Sci. Techn. – Électrotechn. et Énerg., **70**, *4*, pp. 467–472 (2025).
3. Dehiba, M. Abid, A. Aissaoui, *Robust design of power system stabilizer for a single generator-infinite bus power system*, Rev. Roum. Sci. Techn. – Électrotechn. et Énerg., **66**, *4*, pp. 249–253 (2021).
4. A. Chakrabarti, P.K. Sadhu, P. Pal, *A novel dead-time elimination strategy for voltage source inverters in induction heating systems through fractional-order controllers*, Rev. Roum. Sci. Techn. – Électrotechn. et Énerg., **67**, *2*, pp. 181–185 (2022).
5. S. Benaicha, *Robust sensorless speed control of an induction motor drive using a synergetic approach*, Rev. Roum. Sci. Techn. – Électrotechn. et Énerg., **68**, *4*, pp. 381–387 (2023).
6. S. Tahraoui, H. Houari, M. Souaihia, H. Mostefaoui, R. Taleb, E. Bounadja, Y. Mouleloued, *Artificial intelligence features on observations of nonlinear chemical reactor dynamical process*, Rev. Roum. Sci. Techn. – Électrotechn. et Énerg., **70**, *4*, pp. 591–596 (2025).
7. A. Amirullah, A. Adiananda, *Dual fuzzy-Sugeno method to enhance power quality performance using a single-phase dual UPQC-dual PV without DC-link capacitor*, Protection and Control of Modern Power Systems, **9**, pp. 133–153 (2024).
8. I.M.L. Pataro, J.D. Gil, J.D. Alvarez, J.L. Guzman, M. Berenguel, *Robust fractional order PID controller coupled with a nonlinear filtered Smith predictor for solar collector fields*, IFAC-PapersOnLine, **58**, *1*, pp. 234–239 (2025).
9. B. Tomar, N. Kumar, M. Sreejeth, *Robust control of rotary inverted pendulum using metaheuristic optimization techniques based on PID and fractional order PIλDμ controller*, Journal of Vibration Engineering & Technologies, **12**, pp. 1–20 (2024).
10. N. Basil, A.F. Mohammed, B.M. Sabbar, H.M. Marhoon, A.A. Dessalegn, M. Alsharef, E. Ali, S.S.M. Ghoneim, *Performance analysis of hybrid optimization approach for UAV path planning control using FOPID-TID controller and HAOAROA algorithm*, Scientific Reports, **15**, pp. 1–10 (2025).
11. B. Tian, H. Peng, T. Kang, *RBF-ARX model-based predictive control approach to an inverted pendulum with self-triggered mechanism*, Chaos, Solitons & Fractals, **186**, pp. 1–10 (2024).
12. S.M. Ghamari, H. Molaee, M. Ghahramani, D. Habibi, A. Aziz, *Design of an improved robust fractional-order PID controller for buck–boost converter using snake optimization algorithm*, IET Control Theory & Applications, **19**, pp. 1–10 (2025).
13. A.A. Awan, U.S. Khan, A.U. Awan, A. Hamza, *Tracking control and backlash compensation in an inverted pendulum with switched-mode PID controllers*, Applied Sciences, **14**, pp. 1–10 (2024).
14. R. Sekar, M. Arunachalam, K. Subramanian, *Fuzzy-proportional integral derivative controller with interactive decision tree*, Rev. Roum. Sci. Techn. – Électrotechn. et Énerg., **69**, *4*, pp. 395–400 (2024).
15. A. Tahtah, Z. Zahzouh, *Advanced dual-axis solar tracking using a novel artificial neural network-PID control strategy*, Rev. Roum. Sci. Techn. – Électrotechn. et Énerg., **71**, *1*, pp. 39–44 (2026).
16. R. Belal, M. Flitti, M.L. Zegai, *Tuning of PI speed controller in direct torque control of dual star induction motor based on genetic algorithms and neuro-fuzzy schemes*, Rev. Roum. Sci. Techn. – Électrotechn. et Énerg., **69**, *1*, pp. 9–14 (2024).
17. B. Somasundaram, S. Arumugam, *Sliding mode controlled closed loop quadratic boost converter three phase inverter system fed permanent synchronous motor drive with enhanced response*, Rev. Roum. Sci. Techn. – Électrotechn. et Énerg., **70**, *3*, pp. 331–336 (2025).
18. L. Devarajan, S. Chellathurai, *Aquila optimized nonlinear control for DC-DC boost converter with constant power load*, Rev. Roum. Sci. Techn. – Électrotechn. et Énerg., **69**, *4*, pp. 419–424 (2024).
19. M.S. Koupaei Niya, *The effects of hybrid sliding mode learning control and feedforward angle droop controller with high droop gain in hybrid microgrid with load uncertainty and nonlinearity*, Rev. Roum. Sci. Techn. – Électrotechn. et Énerg., **69**, *3*, pp. 277–282 (2024).
20. A. Herizi, R. Rouabhi, F. Ouagueni, A. Zemmit, *Robust wind power control using sliding mode, backstepping, and fuzzy logic*, Rev. Roum. Sci. Techn. – Électrotechn. et Énerg., **70**, *3*, pp. 313–318 (2025).
21. Z. Lammouchi, C. Labiod, K. Srairi, M. Benbouzid, *Enhanced model-free predictive control for voltage source inverters using an adaptive observer*, Rev. Roum. Sci. Techn. – Électrotechn. et Énerg., **69**, *3*, pp. 317–322 (2024).
22. S. Latreche, B. Babes, A. Bouafassa, *Design and real-time implementation of a synergetic regulator for a DC-DC boost converter*, Rev. Roum. Sci. Techn. – Électrotechn. et Énerg., **69**, *3*, pp. 305–310 (2024).